Available online at www.sciencedirect.com
SCIENCE DIRECT
Developmental Biology 275 (2004) 403–421
DEVELOPMENTAL BIOLOGY
www.elsevier.com/locate/ydbio

Nodal inhibits differentiation of human embryonic stem cells along the neuroectodermal default pathway

Ludovic Vallier*, Daniel Reynolds, Roger A. Pedersen

Department of Surgery, University of Cambridge, Cambridge CB2 2QQ, United Kingdom

Received for publication 14 June 2004, revised 12 August 2004, accepted 20 August 2004
Available online 22 September 2004

Abstract

Genetic studies in fish, amphibia, and mice have shown that deficiency of Nodal signaling blocks differentiation into mesoderm and endoderm. Thus, Nodal is considered as a major inducer of mesendoderm during gastrulation. On this basis, Nodal is a candidate for controlling differentiation of pluripotent human embryonic stem cells (hESCs) into tissue lineages with potential clinical value. We have investigated the effect of Nodal, both as a recombinant protein and as a constitutively expressed transgene, on differentiation of hESCs. When control hESCs were grown in chemically defined medium, their expression of markers of pluripotency progressively decreased, while expression of neuroectoderm markers was strongly upregulated, thus revealing a neuroectodermal default mechanism for differentiation in this system. hESCs cultured in recombinant Nodal, by contrast, showed prolonged expression of pluripotency marker genes and reduced induction of neuroectoderm markers. These Nodal effects were accentuated in hESCs expressing a Nodal transgene, with striking morphogenetic consequences. Nodal-expressing hESCs developing as embryoid bodies contained an outer layer of visceral endoderm-like cells surrounding an inner layer of epiblast-like cells, each layer having distinct gene expression patterns. Markers of neuroectoderm were not upregulated during development of Nodal-expressing embryoid bodies, nor was there induction of markers for definitive mesoderm or endoderm differentiation. Moreover, the inner layer expressed markers of pluripotency, characteristic of undifferentiated hESCs and of epiblast in mouse embryos. These results could be accounted for by an inhibitory effect of Nodal-induced visceral endoderm on pluripotent cell differentiation into mesoderm and endoderm, with a concomitant inhibition of neuroectoderm differentiation by Nodal itself. There could also be a direct effect of Nodal in the maintenance of pluripotency. In summary, analysis of the Nodal-expressing phenotype suggests a function for the transforming growth factor-beta (TGF-β) growth factor superfamily in pluripotency and in early cell fate decisions leading to primary tissue layers during in vitro development of pluripotent human stem cells. The effects of Nodal on early differentiation illustrate how hESCs can augment mouse embryos as a model for analyzing mechanisms of early mammalian development.

Keywords: Nodal; TGF-β family; Human embryonic stem cells; Visceral endoderm; Anterior visceral endoderm; Neuroectoderm; Pluripotency; Primary germ layers

Introduction

Human embryonic stem cells (hESCs) are pluripotent cells derived from embryos cultured from the blastocyst stage (Thomson et al., 1998). Their embryonic origin confers upon hESCs the capacity to differentiate into the three primary germ layers as well as extraembryonic tissues (Xu et al., 2002). This property of pluripotency is maintained even after prolonged periods of in vitro culture. hESCs also have a prolonged proliferative capacity and genetic stability that is unique for cultured human cells (Amit et al., 2000). These characteristics confer an exceptional value on hESCs for regenerative medicine. Robust technologies for enhancing and diminishing gene function in hESCs are now becoming available to expedite their controlled in vitro differentiation into specific, clinically valuable cell types (Vallier et al., 2004). Beyond this

* Corresponding author. Department of Surgery, University of Cambridge, Cambridge Institute for Medical Research, Hills Road, Cambridge CB2 2XY, United Kingdom.
E-mail address: lv225@cam.ac.uk (L. Vallier).

0012-1606/$ - see front matter © 2004 Elsevier Inc. All rights reserved.
doi:10.1016/j.ydbio.2004.08.031

potential for clinical applications, hESCs also represent a unique in vitro system for modeling early human development at stages, such as gastrulation, that have heretofore been studied only in laboratory mammals.

The first event of gastrulation in mouse is the formation of the primitive streak (Lu et al., 2001). This distinct morphological structure marks the posterior pole of the embryo's anteroposterior (A–P) axis and also generates mesendoderm, the source of definitive mesoderm and endoderm. Recent studies have revealed that extraembryonic tissues are essential for A–P patterning. Visceral endoderm (VE) in particular is involved in the establishment, localization, and orientation of the anterior pole of the A–P axis (Kalantry et al., 2001; Kimura et al., 2000). Specifically, the anterior visceral endoderm (AVE) is essential for correct development of the trunk and head (Hallonet et al., 2002; Perea-Gomez et al., 2001a; Varlet et al., 1997). Although understanding of the molecular basis of A–P patterning in mammalian development is still limited, initial studies have revealed a key role of the transforming growth factor-beta (TGF-β) growth factor superfamily member, Nodal.

Genetic studies have shown that disruption of Nodal signaling in mouse embryonic development inhibits primitive streak formation (Conlon et al., 1994; Zhou et al., 1993) and blocks AVE maturation (Robertson et al., 2003). Like other TGF-β superfamily members, Nodal binds to heteromeric complexes between type I (Alk4 and Alk7) and type II (ActRIIB) Activin receptors, which in turn act through the Smad2/Smad3 signaling pathway (reviewed in Schier, 2003). Nodal signaling is also regulated by Cripto, an extracellular GPI-linked protein which acts as a cofactor, and by antagonists, the best studied of which are Lefty1 and Cerberus. These antagonists are expressed during gastrulation in the AVE and in anterior definitive endoderm (ADE), where they act to diminish Nodal activity in the embryo's anterior, thus preserving this region for head development (Perea-Gomez et al., 2001b). The abnormalities of mouse Nodal mutants at the early primitive streak and subsequent stages emphasize the importance of this genetic pathway in early mammalian development, a role that has been generalized to vertebrates in *Xenopus* and zebrafish studies (reviewed in Schier, 2003). Thus, the essential functions of Nodal signaling in the differentiation of the primary germ layers and in A–P patterning seem to be evolutionary conserved.

The key function of Nodal in mesoderm and endoderm differentiation would appear to designate it as a candidate to drive in vitro differentiation of hESCs into these primary germ layers, which are particularly attractive for clinical application as sources of potentially transplantable cell types. We therefore investigated the function of Nodal signaling during hESC differentiation by adding recombinant Nodal or by overexpressing the Nodal gene. We found that, rather than inducing differentiation of hESCs into the mesoderm and endoderm primary germ layers, Nodal inhibited progression along the neuroectoderm default pathway of neuroectoderm while promoting the differentiation of extraembryonic visceral endoderm and maintaining the expression of markers of pluripotency.

Materials and methods

hESC culture and transfection

H9 hES cells (WiCell, Madison, WI) were cultured as described (Thomson et al., 1998) in KSR medium containing KO-DMEM supplemented with Serum Replacement (Invitrogen). Every 4 days, cells were harvested using 1 mg/ml collagenase IV (Gibco) and then plated into 60-mm plates (Costar) precoated with 0.1% porcine gelatin (Sigma) and containing 1×10^5 irradiated mouse embryonic fibroblasts. For stable transfection with vectors encoding mouse Nodal or NodalGFP, three confluent 60-mm plates containing around 2000 hES colonies each were plated onto one six-well gelatin-coated plate containing 5×10^4 feeders. After 48 h, the cells were transfected using Lipofectamine 2000 (Invitrogen) as described (Vallier et al., 2004). Three days after transfection, the cells were passed onto 60-mm gelatin-coated tissue-culture plates containing puromycin-resistant mouse fetal fibroblasts as feeders. After 3 additional days, puromycin (1 μg/ml final concentration) was added. Puromycin-resistant colonies that appeared by 12 days of selection were picked, dissociated, and plated onto 24-well gelatin-coated, feeder-containing plates, and expanded for further analysis as described above.

hESC differentiation was induced by embryoid body (EB) formation. This was accomplished by incubating colonies in medium containing 1 mg/ml collagenase IV without FGF for 6 h, after which all the colonies (but not feeders cells) had detached from the plate. The colonies were then rinsed once in the corresponding medium to be used for differentiation (below) and grown in nonadherent conditions to generate EBs. The composition of the medium used for differentiation was either (1) KO-DMEM supplemented by 10% fetal bovine serum (FBS; Hyclone), (2) KO-DMEM supplemented by 20% Serum Replacer (Gibco), or (3) chemically defined medium (CDM) (Johansson and Wiles, 1995) consisting of 50% IMDM (Gibco) plus 50% F12 NUT-MIX (Gibco), supplemented with 7 μg/ml of insulin (Roche), 15 μg/ml of transferrin (Roche), 450 μM of monothioglycerol (Sigma), and 5 mg/ml albumin fraction V (Sigma). The effect of Nodal on EB growth was assayed by adding 50 ng/ml of mouse recombinant Nodal (R&D systems).

To obtain outgrowths of Nodal-expressing EBs in adherent conditions, they were plated in six-well plates after 10 days of differentiation as EBs. To allow EB adhesion in CDM, plates were precoated with FBS for 24 h at 37°C and then washed twice in PBS to eliminate any serum. Plated EBs were then grown for 20 additional days in CDM.

Karyotype analyses were performed on H9 and hSF-6 cells at various passages. Abnormalities involving chromosomes 9, 5, and 19 were observed at late passages (p80–p115) confirming recent results suggesting that hESCs are susceptible to genetic instability (Draper et al., 2004). Consequently, only hESCs from earlier passages (p50–p70) were used for these experiments. Nodal-expressing clones were found to have a normal karyotype during at least 15 passages after subcloning.

Flow cytometry

NodalGFP-overexpressing hESCs were dissociated with trypsin (0.25%) plus EDTA (1 mM; Gibco), washed once in medium containing fetal calf serum (PAA), and washed twice in PBS containing 0.1% serum (hES). The cells were then immediately analyzed on a FACSCalibur flow cytometer (Becton Dickson) using Cellquest acquisition and analysis software (Becton Dickson).

For detection of SSEA-4, adherent cells were washed twice in PBS then incubated for 20 min at 37°C in cell dissociation buffer (Invitrogen). Cells were then dissociated by gentle pipetting and resuspended at approximately 0.1 to 1.0 × 10^5 cells/ml in PBS + 3% normal goat serum containing 0.1% azide (NGS) (Serotec). Cells were incubated for 20 min at 4°C with SSEA-4 antibody (clone MC813, 1:200, Developmental Studies Hybridoma Bank) or the corresponding isotype control (mouse IgG isotype control, Pharmingen). Cells were then washed twice in PBS + 3% NGS and incubated for 20 min on ice with an fluorescein isothiocyanate (FITC)-conjugated goat anti-mouse IgG antibody (1:250, Sigma) and subsequently resuspended in PBS + 3% NGS for stained with 7-aminoactinomycin D (7-AAD) viability dye (Immunotech) at 20 μl/ml for 15 min at room temperature. Live cells identified by 7-AAD exclusion were analyzed for surface-marker expression using FACSCalibur.

Transcriptional response assay

DNA plasmids including the pAR3-lux firefly luciferase reporter and CMV-Renilla (Promega) were cotransfected into hESCs to assess their transcriptional response to exogenous Nodal. The ratio between pAR3-lux and CMV-Renilla was 10:1. recNodal or supernatant of Nodal-overexpressing hESCs (collected after 24 h of culture) was added 18 h after pAR3-lux transfection. Cells were harvested 48 h later for luciferase essay. Luciferase activity was measured using the dual luciferase assay in cell lysates as described (Promega). Firefly luciferase activity was normalized to Renilla luciferase activity.

RNA extraction and RT–PCR

Total RNAs were extracted from hESCs or EBs using the RNeasy Mini Kit and RNeasy Microkit for dissected EB layers (Qiagen). Each sample was treated with RNAse-Free DNAse (Qiagen) to avoid DNA contamination. A test PCR was done on all the RNA samples to verify the absence of genomic contamination. For each sample, 0.5 μg of total RNA was reverse-transcribed using Superscript II Reverse Transcriptase (Invitrogen). PCR reaction mixtures were prepared as described (Promega protocol for Taq polymerase) then were denatured at 94°C for 5 min and cycled at 94°C for 30 s, 50–65°C for 30 s, and 72°C for 30 s followed by final extension at 72°C for 10 min after completion of 40 cycles. Primer sequences, annealing temperatures, and their expected products are described in Supplementary Table 1. All the PCR reactions were done with a negative control containing only water and a positive control containing RNA extracted from EBs grown for 30 days in FBS-supplemented medium (data not shown). The expression of the beta2 microglobulin (β2M) housekeeping gene was used to normalize PCR reactions.

Immunofluorescence and histology

hESCs or their differentiated derivatives were fixed for 20 min at 4°C in 4% paraformaldehyde (PFA) and then washed three times in PBS. Cells were incubated for 20 min at room temperature in PBS containing 10% goat serum (Serotec) and subsequently incubated for 2 h at room temperature with primary antibody diluted in 1% goat serum in PBS as follows: SSEA-1 (clone MC480, 1:50, Developmental Studies Hybridoma Bank), SSEA-4 (clone MC813, 1:50, Developmental Studies Hybridoma Bank), Tra-1-60 (Chemicon International, 1:20), Oct-4 (SantaCruz, 1:100), and alphafetoprotein (αFP, R&D systems, 1:200). Cells were then washed three times in PBS and incubated with fluorescein isothiocyanate-conjugated antimouse IgG or IgM (Sigma 1:200 in 1% goat serum in PBS) for 2 h at room temperature. Unbound secondary antibody was removed by three washes in PBS. Hoechst 33258 was added to the first wash (Sigma 1:10,000).

For cryosectioning, EBs were fixed overnight at 4°C in PBS with 4% PFA and then incubated overnight in PBS with 30% sucrose. After freezing on dry ice in Tissue-Tek OCT medium (Sakura), EBs were sectioned at 5–7 μm, deposited on polylysine-coated slides, and stored at 4°C. Slides were postfixed in PBS containing 4% PFA for 20 min on ice. Immunostaining was performed following the same procedure used for plated cells (above). Secondary antibody was Cy3-conjugated donkey antimouse (Chemicon International, 1:500). Specimens were mounted in Pro-Long antifade medium (Molecular Probes).

In situ hybridization

In situ hybridization (ISH) of hESC colonies and EBs was performed using the method described by Streit and Stern (2001). Antisense and sense probes for Oct-4, HNF3b, Brachyury, Cerberus, Nodal, and H19 were synthesized

using the DIG RNA labeling kit form Roche. Each probe was generated by subcloning PCR fragments synthesized using the corresponding primers (see Supplementary Table 1) in the Topo cloning PCRII vector (Invitrogen).

Results

hES cells and their differentiated derivatives express components of the Nodal pathway

We first tested expression of Nodal signaling components and pluripotency markers in hESCs using semiquantitative RT–PCR (Fig. 1A). This assessment detected Nodal, Cripto, ActRIIB, and Alk4, components of the Nodal signaling pathway, as well as Oct-4 and FGF4, two markers of pluripotency (Avilion et al., 2003). Nodal expression in hESCs was confirmed by in situ hybridization (ISH) (Fig. 1B). We then tested expression of these genes during differentiation of hESCs into embryoid bodies (EBs) (Fig. 1A). Nodal and Cripto transcripts disappeared after 6 days of differentiation, this coinciding with the loss of transcripts for Oct-4 and FGF4. Nodal receptor (Alk4, ActRIIB) expression was maintained during this period of differentiation. These results are consistent with previous data showing expression of different TGFβ pathway components in hESCs and during differentiation (Brandenberger et al., 2004; Brivanlou et al., 2003; Ginis et al., 2004; Schuldiner et al., 2000; Zeng et al., 2004). The expression of Nodal and its receptors implicates the Nodal signaling pathway as a potential factor involved in regulating the development of hESCs and their differentiated derivatives.

As a basis for determining the role of Nodal in hESC development, we examined the effect of growth media supplemented with protein components of varying complexities. No major differences in the expression of Nodal pathway components were observed between media containing fetal bovine serum (FBS), serum replacer (SR), or neither of these (chemically defined medium, CDM) (Johansson and Wiles, 1995). Therefore, we elected to use CDM in the remaining experiments to avoid the presence of unknown factors that could interfere with the Nodal signaling pathway.

The expression of markers representative of the definitive germ layers (ectoderm, mesoderm, and endoderm) was also studied to evaluate the capacity of hESCs for differentiation in this system. Markers of the neuroectoderm lineage, including Pax6, MAP2, Sox1, Sox2, Musashi, Hesx1, Nestin, and Neurod1 were all expressed in EBs grown in CDM (Fig. 2B and data not shown). Markers of mesoderm differentiation, including Myf5 and MyoD (reviewed in Parker et al., 2003), were detected but only transiently (Fig. 2B), suggesting that CDM alone was permissive but not inductive of definitive mesoderm differentiation. Previous data predict such a response to CDM, since addition of BMP4 or Activin was required to induce mesoderm differentiation of mouse ES cells in CDM (Wiles and Johansson, 1999). There was no expression of the definitive endoderm marker intestinal fatty acid binding protein (IFABP) (Fig. 2B) (Wells and Melton, 2000). However, expression of

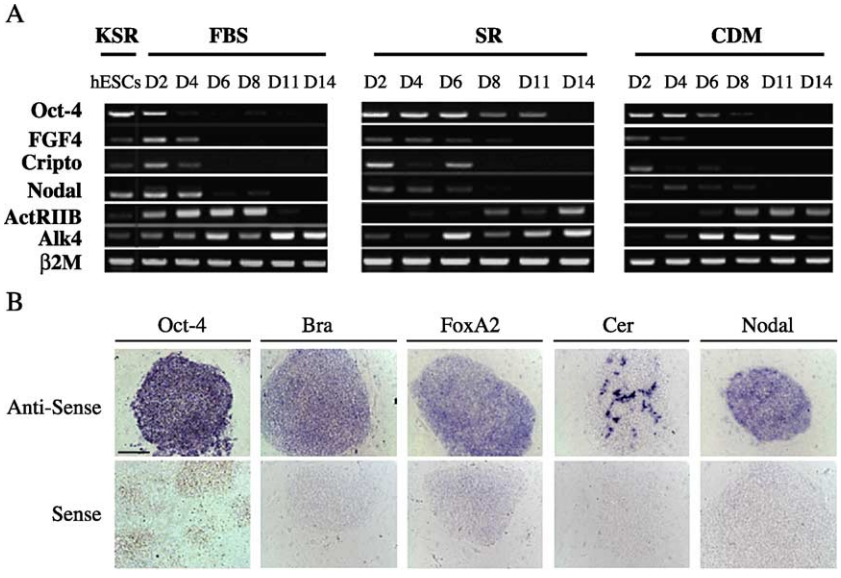

Fig. 1. Expression of markers of pluripotency, gastrulation, and the Nodal pathway in hESCs and their differentiated derivatives. (A) Examination of pluripotency markers and Nodal pathway components in hESCs (box, left) and during differentiation using RT–PCR. hESCs were initially grown in KSR medium on a feeder layer (see Materials and methods). Differentiation was induced by growing hESCs as EBs for varying times using three different media. FBS, medium containing 10% fetal bovine serum; SR, medium containing 20% serum replacer; and CDM, medium containing BSA, but without serum or serum replacer. RNAs were extracted every 2 or 3 days for 2 weeks (D2–D14), and then RT–PCR analysis was performed to detect the expression of the genes denoted. (B) Examination of pluripotency (Oct-4) and gastrulation markers Brachyury (Bra), Foxa2, and Cerberus (Cer) plus Nodal in undifferentiated hESCs using in situ hybridization (ISH). Sense probes were used as negative controls. Scale bar: 200 μm.

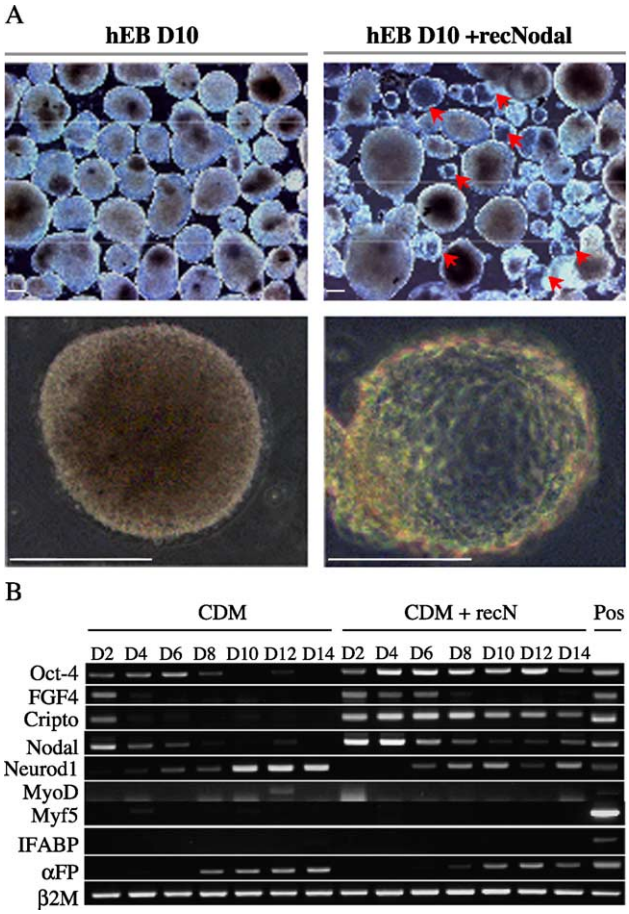

Fig. 2. Effect of recNodal on hESCs differentiation. (A) EBs grown for 10 days in the absence (hEB D10, upper left panel) or presence of recNodal (hEB D10 + recNodal, upper right panel). The lower left panel illustrates at higher magnification a typical EB obtained in CDM. The lower right panel illustrates at higher magnification an embryoid body developing in recNodal. EBs grown in the presence of recNodal frequently contained hollow and distended vesicles (indicated by red arrowheads in upper right panel). Scale bar: 200 μm. (B) Expression of pluripotency and differentiation markers during differentiation of hESCs in the absence or presence of recNodal. RNAs were extracted every 2 days during 14 days (D2–D14), and then RT–PCR analysis was performed to detect the expression of the genes denoted. EBs differentiated for 30 days in medium containing serum were used as positive control (Pos).

extraembryonic endoderm markers, including alpha-fetoprotein (αFP) (Fig. 2B) and GATA4 (data not shown) (Krumlauf et al., 1985; Narita et al., 1997), was observed, suggesting that CDM is permissive for differentiation of hESCs into a component of the primitive endoderm lineage. Taken together, these results suggest that growing hESCs in CDM in the absence of the growth factors provided by complex protein mixtures favors differentiation into the definitive neuroectodermal but not the definitive mesodermal or endodermal lineages. This finding is therefore consistent with the neuroectoderm default model that has been described for the *Xenopus* embryo and postulated to exist in embryonic stem cells (Parisi et al., 2003; Tropepe et al., 2001; reviewed in Munoz-Sanjuan and Brivanlou, 2002).

We also examined hESC colonies for their expression of early markers of gastrulation, including Brachyury (Bra), Foxa-2 (HNF3β), and Cerberus (Cer). Surprisingly, we detected the expression of these three genes in undifferentiated hESCs by RT–PCR (data not shown). The distribution of transcripts was further examined using in situ hybridization (Fig. 1B). Similarly to Nodal, Bra and Foxa-2 transcripts were detected in all the colonies (the expression of the corresponding proteins was not investigated due to the unavailability of the respective antibodies). In the same cultures, Oct-4 displayed a similar pattern of ubiquitous expression. By contrast, Cer expression was limited to a small number of cells scattered throughout a fraction of the colonies. These results revealed that transcription of genes commonly used to study gastrulation in mouse embryos could not be used as markers for hESC differentiation. Therefore, we selected markers for gastrulation and primary germ layer differentiation that were not expressed in hESCs. These consisted of Neurod1 for neuroectoderm differentiation (Breslin et al., 2003), MyoD and Myf5 for mesoderm differentiation, IFABP for definitive endoderm differentiation, and αFP for extraembryonic endoderm differentiation.

Recombinant Nodal modulates differentiation of hESCs grown as embryoid bodies

We first determined the effect of Nodal as an inducer of hESC differentiation by adding recombinant Nodal (recNodal) to colonies in monolayer cultures. After 6 days in recNodal (50 ng/ml), colony morphology was normal (data not shown), with no additional differentiation observed as compared to untreated cells. Consistent with this, addition of recNodal led neither to decreased expression of Oct-4 or FGF4 nor to increased expression of NeuroD1, MyoD, or αFP (data not shown).

We next analyzed the Nodal effect on differentiation by adding recombinant Nodal to hESCs cultured as embryoid bodies. Control EBs generated from hESCs grown in CDM were typically round, homogenous, and compact (Fig. 2A). By contrast, EBs developing in CDM containing recNodal (50 ng/ml) acquired a cystic morphology (Fig. 2A). Expression of pluripotency and differentiation markers was analyzed by semiquantitative RT–PCR every 2 days during 2 weeks of culture (Fig. 2B). Expression of Oct-4, Cripto, and endogenous Nodal persisted in EBs grown in the presence of recombinant Nodal. Despite the Nodal-induced persistence of expression for these markers of pluripotency, expression of the neuronal marker Neurod1 was also detected, and expression of FGF4 (a marker of pluripotency that is sensitive to differentiation-induced silencing; our unpublished observations) disappeared within 1 week. However, expression of the definitive mesoderm (MyoD and Myf5, Fig. 2B) and endoderm markers (IFABP, Fig. 2B) was not seen in cultures containing recNodal, although they did appear in controls. Expression of the

extraembryonic endodermal marker αFP was strongly induced in both Nodal-treated and control EBs, suggesting that extraembryonic endoderm differentiation was occurring in both conditions. Taken together, these gene expression findings indicate that recombinant Nodal modulates the differentiation of hESCs grown as EBs. However, EBs are compact aggregates of cells and have epithelial differentiation of their outer cells. Consequently, the internal diffusion of exogenously added growth factor is likely to be limited, and this could account for the diversity of molecular features (expression of both pluripotency and differentiation markers) noted during EB development accompanying treatment with recNodal.

Generation of Nodal-overexpressing hESC lines

To overcome the limitations of exogenously added growth factors, we undertook to overexpress Nodal stably in hESCs, using an approach we had developed for such purposes (Vallier et al., 2004). Secretion and maturation of Nodal protein involve proteolytic processing (Constam and Robertson, 1999). Accordingly, we used not only the native Nodal coding sequence (NHN), but also a modified version in which the native proregion was replaced by the BMP 2/4 proregion (BHN, Fig. 3A), which is known to be processed effectively in a large number of cell types (Dale et al., 1993; Thomsen and Melton, 1993). Finally, to enable an easy monitoring of Nodal protein expression, we alternatively used a fusion gene between mouse Nodal cDNA and the green fluorescent reporter gene (NodalGFP) (Sakuma et al., 2002). Briefly, mouse Nodal cDNAs (NHN, BHN, or NodalGFP, Fig. 3A) were subcloned into the pTP6 expression vector (Pratt et al., 2000), and the resulting constructs were transfected in both H9 and hSF-6 hES cell lines. Colonies generated using the NHNpTP6 vector (N = 25 for H9 cell line and N = 8 for hSF-6 cell line) and the BHNpTP6 vector (N = 5 for H9 cell line and N = 8 for hSF-6 cell line) were screened for Nodal expression using semiquantitative PCR with primers that distinguished the mouse Nodal cDNA from its human counterpart (Fig. 3B). Colonies generated using the NodalGFPpTP6 (N = 15 for hSF-6) were screened using FACS to allow a quantitative and qualitative evaluation of NodalGFP protein expression (Fig. 4B). These analyses showed clear evidence of Nodal protein expression and also revealed important variations in its level between different cell lines. We then established a reporter assay for Nodal signaling activity to evaluate its proper secretion. H9 cells incubated with RecNodal or with supernatant from Nodal-overexpressing hESC cell lines were transitorily transfected with the pAR3-lux reporter, which contains an Activin response element from the *Xenopus* Mix.2 gene (Hayashi et al., 1997). The pAR3-lux reporter plasmid has previously been shown to be inducible by Nodal and Activin in embryonal carcinoma cells (Kumar et al., 2001). Incubation of pAR3lux reporter-transfected H9 cells in RecNodal (50 ng/ml) resulted in a 4-fold induction as compared to control (P = 0.01, 4 d.f.) (Fig. 3C), and incubation in supernatant of a representative Nodal-overexpressing hESC cell line resulted in 20-fold induction above control level (P = 0.01, 4 d.f.) (Fig. 3C). Therefore, functional Nodal protein is properly expressed and secreted by hESCs. Finally, five Nodal-expressing H9 cell lines (NHN4, NHN5, NHN13, NHN14, BHN1, and BHN2) and five Nodal-expressing hSF-6 cell lines (NHN1hsf6, NHN4hsf6, BHN1hsf6, NodalGFP3hSF6, and NodalGFP7hSF6) were studied to verify that the results obtained were cell line-and clone-independent (Supplementary Figs. 1A, B). Moreover, an hrGFP-overexpressing hESC cell line was included as a negative control with wild-type hESCs in each of the experimental series to control for any effects induced by the genetic manipulation procedure itself.

These Nodal-expressing cell lines and their respective controls were characterized as monolayer cultures for the expression of the pluripotency markers Oct-4, Tra-1-60, and SSEA-4 using immunofluorescence (Henderson et al., 2002). No differences were observed as compared to wild-type hESCs (Fig. 3D). Moreover, the hESC differentiation marker SSEA-1 was not detected (data not shown). Gene expression was assessed using RT–PCR, which confirmed that Nodal-expressing hESCs expressed the same pluripotency markers as wild-type cells without expressing the markers of differentiation, Neurod1, MyoD, Myf5, IFABP, and αFP (Supplementary Figs. 1 and 2, and data not shown). Therefore, Nodal overexpression did not induce primary germ layer differentiation of hESCs grown as monolayer cultures, confirming and expanding the results we obtained with recombinant Nodal.

Fig. 3. Effect of Nodal overexpression on hESCs. (A) Map of the NHNpTP6 and BHNpTP6 vectors. pTP6 vector contains the CAGG promoter followed by the Nodal cDNA and an IRES puromycin resistance gene allowing strong selection for transgene expression. (B) Screening of Nodal-expressing hESCs. Expression of mouse Nodal in H9 sublines generated by transfection of HNHpTP6, as determined by RT–PCR. RNA from hESCs expressing a gene encoding green fluorescent protein (hrGFP2) and nontransfected hESCs were used as negative controls. β2 Microglobulin (β2M) was used as a loading control. (C) RecNodal and supernatant of Nodal-expressing hESCS cells activate the pAR3-lux reporter. H9 cells were transiently transfected with the p3AR-Lux vector. After transfection, cells were incubated 48 h in the absence (Neg) or presence of 50 ng/ml of recNodal, or in presence of supernatant from a representative Nodal-overexpressing hESC line (SupNHN4). Normalized luciferase activity is expressed as the mean ± SD from three informative experiments. (D) Expression of pluripotent stem cell markers by wild-type H9 cells and Nodal-expressing hESCs. SSEA4, Tra-1-60, and Oct-4 expression were analyzed in wild-type cells and in Nodal-expressing cells by immunofluorescence. White arrows in the left panels indicate regions with a differentiated morphology frequently seen in wild-type colonies but absent from those expressing Nodal. Such areas were negative for the expression of Oct-4, Tra-1-60, and SSEA4 (green fluorescence) showing the specificity of these markers. Scale bar: 200 μm.

Altered morphogenesis of Nodal-expressing EBs

We then investigated the development of EBs generated from Nodal-expressing hESC by growing colonies in suspension cultures using CDM medium. As previously noted, control EBs grown in CDM developed almost entirely as homogenous spheres with no apparent tissue organization. By contrast, the majority of Nodal-expressing EBs (type 1) consisted of three distinct cell layers (nEB1, Fig. 4A; and NoGFP, Fig. 4B). The outside layer (L1, Fig.

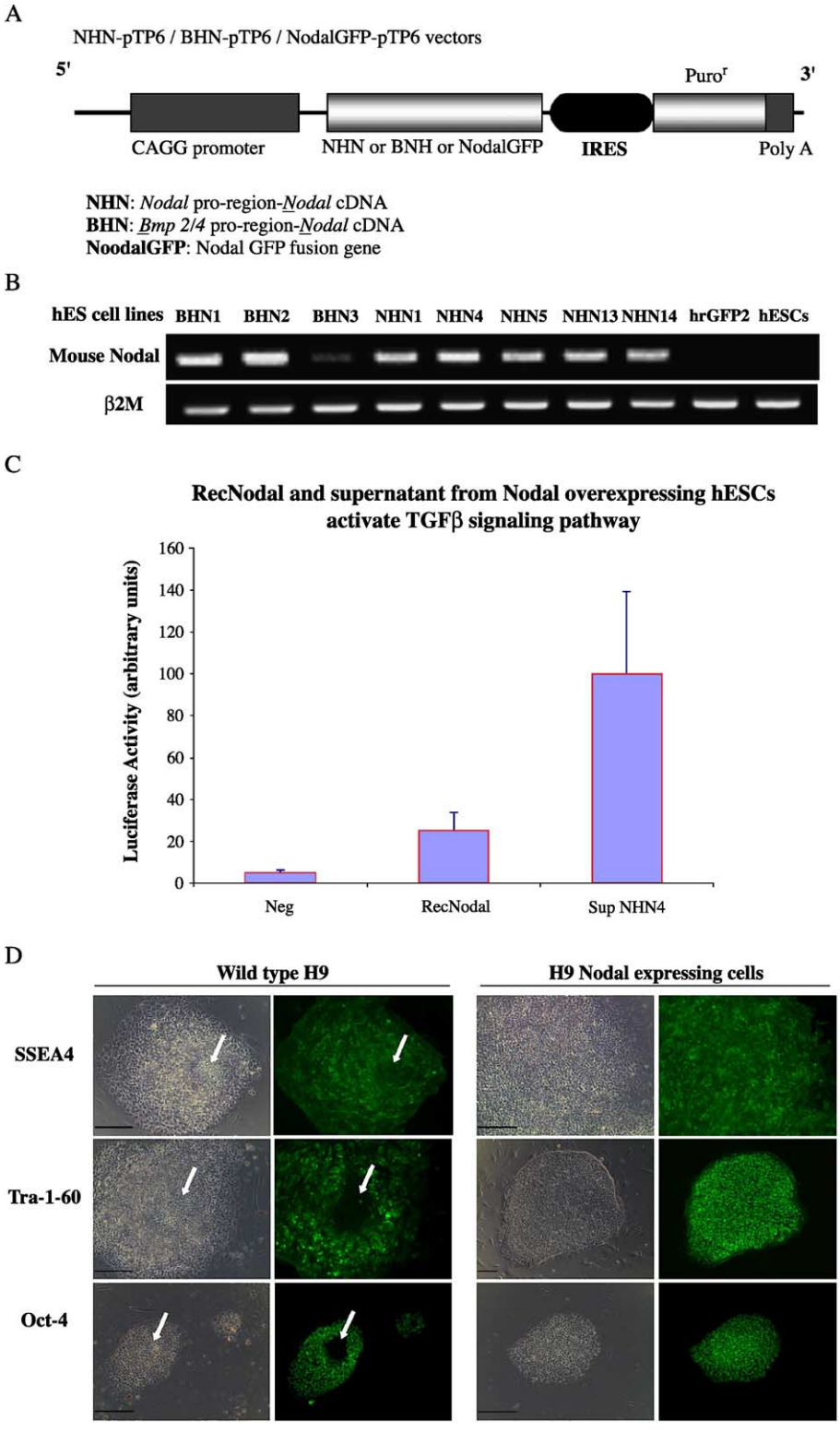

4A) of type 1 EBs was a single, thin sheet of cells. The inside layer (L2) consisted of cells organized into a columnar epithelium, which strikingly resembled the epiblast layer of early postimplantation stage mouse embryos, whereas the central core (L3) contained rounder cells. Several other types of Nodal-expressing EBs were also observed, but at substantially lower frequencies. EBs with type 2 morphology (nEB2, Fig. 4A) consisted of a single

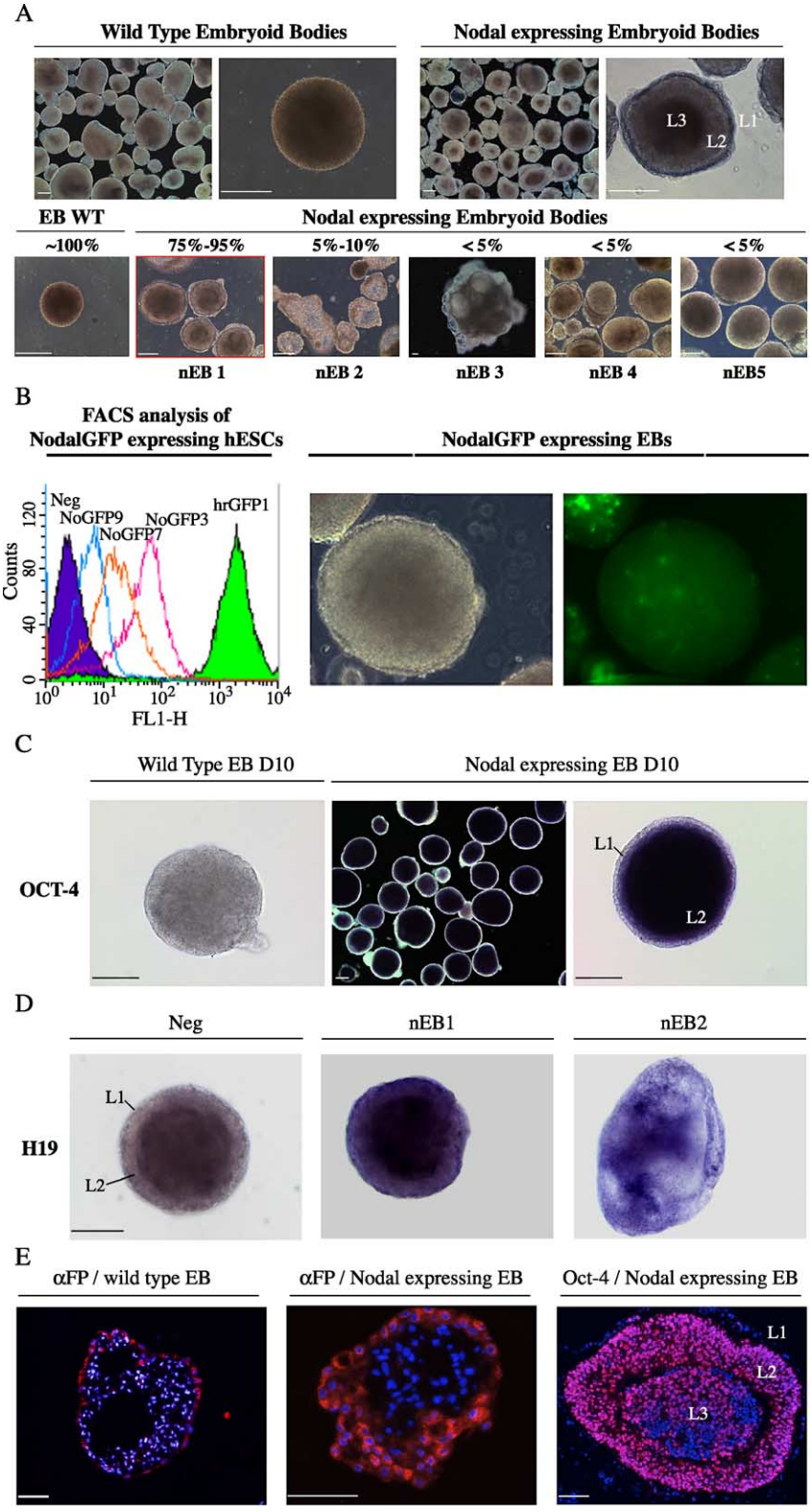

sheet of cells surrounding an empty cavity. EBs with type 3 morphology (nEB3, Fig. 4A) developed to a more prominent size, yet lacked an organized structure. EBs with type 4 morphology (nEB4, Fig. 4A) were asymmetric, having one side that resembled the homogenous control EBs and a distinct opposite side consisting of an outer cell layer (L1) in contact with a columnar epithelial layer (L2) like that seen in type 1 EBs. Finally, homogenous EBs (type 5) similar to wild-type EBs were seen at a low frequency (nEB5, Fig. 4A). The fraction of type 1 EBs (ranging between 75% and 95%) appeared to depend on the quantity of EBs and the size of the hESC colonies used to generate EBs. A high density of EBs (3000 EBs/15 ml of CDM) decreased the fraction of type 1 EBs. The use of small colonies (<30 cells) appeared to increase the fraction of type 2 EBs. Moreover, hESCs expressing a very low level of NodalGFP (NoGFP9, Fig. 4B) produced a majority of EBs that were similar to wild type (type 5), indicating that formation of type 1 EBs depends on the level of Nodal expression. In sum, Nodal-expressing hESCs underwent a unique developmental program during EB formation, resulting in differentiation of novel EB morphologies and cellular phenotypes as compared with control EBs.

Nodal-overexpressing EBs display markers of pluripotency and extraembryonic endoderm

We therefore undertook a molecular and immunohistochemical analysis to determine the identity of cells in the complex embryoid bodies generated by Nodal-expressing hESC. RT–PCR analysis performed on each of the EB types (Table 1) revealed that the pluripotency markers Oct-4, FGF4, and Cripto continued to be expressed in types 1, 3, 4, and 5 EBs after 10 days of differentiation, in contrast to control EBs, which had essentially ceased expressing pluripotency markers within 1 week of differentiation in CDM (Fig. 2B). Oct-4 expression in Nodal-expressing EBs was confirmed at the RNA level by in situ hybridization and at the protein level by immunofluorescence (Figs. 4C, E). No expression of neuroectoderm markers (Table 1, NeuroD1) was detected in Nodal-expressing EBs, in contrast to control EBs, which did express them (Table 1, WT-EB). Thus, Nodal expression during EB development led to retained expression of markers of pluripotency, while preventing progression along the default neuroectoderm pathway, a principal endpoint of differentiation in controls.

Nodal expression during the development of EBs did not block differentiation altogether, as indicated by evidence for the formation of an extraembryonic cell type. In type 1 EBs, we detected expression by RT–PCR of a set of markers characteristic of mouse extraembryonic endoderm, including αFP, BMP2, GATA4, HNF3β, and HNF4 (Table 1). Transcripts of H19, an imprinted gene strongly expressed in extraembryonic tissues at the time of gastrulation in mouse embryos (Poirier et al., 1991), were also detected by in situ hybridization (Fig. 4D). In addition, the presence of αFP protein was detected in type 1 Nodal-expressing EBs using immunofluorescence (Fig. 4E). Type 2 Nodal-expressing EBs also expressed a similar set of marker genes, specifically, αFP, BMP2, HNF3β H19, HNF4, Nodal, and GATA4 (Table 1, Fig. 4D). The only known candidate for a tissue expressing this set of genes during early mammalian development is the visceral endoderm (VE), which becomes fully differentiated at the time of gastrulation in the mouse embryo. Consistent with this, neither type 1 nor type 2 Nodal-expressing EBs expressed the definitive endoderm marker, IFABP (Table 1). Moreover, the αFP gene was the only member of the set of visceral endoderm markers that was detected in the control EBs at this time of differentiation, suggesting that control EBs progress only a limited way on the pathway towards extraembryonic endoderm (Table 1, Fig. 4E). Therefore, Nodal expression apparently induces the differentiation of VE in the vast majority of EBs developing from Nodal-expressing hESC.

Nodal-expressing EBs consist of an outer layer of AVE-like cells surrounding an inner layer of epiblast-like cells that maintain the molecular signature of pluripotency

The developmental consequences of Nodal expression were further investigated by examining the constituent layers of Nodal-expressing EBs. RT–PCR analysis of microdissected tissues of type 1 EBs revealed that the outside layer (Table 1, L1) expressed markers of visceral

Fig. 4. Effect of Nodal overexpression on differentiation of hESCs. (A) Morphology of wild-type EBs and Nodal-expressing EBs undergoing differentiation during 10 days in CDM. Almost all the wild-type EBs grown in CDM were solid, homogenous masses of cells (typical EBs shown in the upper left panels). By contrast, the vast majority of Nodal-expressing EBs were organized into three layers (upper right panels) denoted as layers L1 (outer), L2 (inner), and L3 (central core). The bottom panels show the frequency distribution of wild-type and Nodal-expressing EBs into distinct morphological types (nEB1 to nEB5). Scale bar: 200 μm. (B) NodalGFP protein expression in hESCs and in differentiated EBs. FACS analysis of NodalGFP-expressing hESCs (left panel) showed a clear expression of Nodal protein. Wild-type cells were used as negative control (Neg), whereas an hrGFP-overexpressing cell line was used as positive control (hrGFP1). Three NodalGFP-expressing cell lines (NoGFP3, NoGFP7, and NoGFP9) of 15 generated were used for this experiment. NodalGFP-expressing EBs (middle and left panel) were also organized into three layers as observed for expression of NHN and BHN Nodal transgene expression. (C) Analysis of Oct-4 expression after 10 days of differentiation in wild-type EBs (left panel) and Nodal-expressing EBs (middle and right panels) using in situ hybridization. Oct-4 was invariably detected in the inner layer (L2) of type 1 Nodal-expressing EBs (nEB1), but it was consistently absent from the outside layer (L1, right panel). Scale bar: 200 μm. (D) Analysis of H19 gene expression after 10 days of differentiation in types 1 and 2 Nodal-expressing EB (nEB1 and nEB2) using in situ hybridization. Sense probe was used in the negative control (Neg) to show absence of nonspecific staining. Scale bar: 200 μm. (E) Immunofluorescence analysis of αFP and Oct-4 expression after 10 days of differentiation in wild-type (left panel) and Nodal-expressing EBs (middle and right panels). Nuclei are shown by Hoechst staining (blue fluorescence). Visceral endoderm is indicated by αFP expression (red fluorescence, left and middle panels). Pluripotent cells in Nodal-expressing EBs are shown by Oct-4 expression (pink florescence combining red Oct-4 + blue nuclear staining, right panel) Scale bar: 50 μm.

Table 1
Gene expression patterns of wild-type and Nodal-expressing EBs

Tissue	Markers	WTEB	nEB1	nEB2	nEB3	nEB4	nEB5	L1	L2	L3
hESCs	Oct-4	–	+	–	+	+	+	–	+	+
	FGF4	–	+	–	+	+	+	–	+	+
	Cripto	–	+	+	+	+	+	nd	nd	nd
Ecto	Neurod1	+	–	–	–	–	+	–	–	–
Meso	Bra	–	+	–	+	+	+	nd	nd	nd
	MyoD	–	–	–	–	–	–	–	–	–
	MyF5	–	–	–	–	–	–	–	–	–
Endo	IFABP	–	–	–	–	–	–	–	–	–
	HNF3	–	+	+	+	+	+	+	+	+
VE	AFP	+	+	+	+	+	+	+	–	–
	HNF4	–	–	+	+	–	–	nd	nd	nd
	H19	–	+	+	+	+	+	+	–	+
	GATA4	–	+	+	+	+	+	+	–	–
	BMP2	–	+	+	+	+	+	nd	nd	nd
	hNODAL	–	+	+	+	+	+	+	+	+
AVE	HEX	–	+	–	+	+	+	+	–	–
	Cer	–	+	–	+	+	+	+	+	+
	Lhx1	+	+	–	+	+	+	+	+	+
	Otx2	–	+	–	+	+	+	+	+	+

The expression of markers characteristic of hESCs, ectodermal (ecto), mesodermal (meso), or endodermal (endo) germ layers, and visceral (VE) or anterior visceral (AVE) extraembryonic endoderm was analyzed after 10 days of differentiation using RT–PCR. Results are summarized for wild-type EBs (WTEB), nodal-expressing EB (types nEB1, nEB2, nEB3, nEB4, and nEB5), and the three layers of nEB1 (L1, L2, and L3). Expression of markers is indicated by (+). Expression of Cripto, Brachyury (Bra), HNF4, and BMP2 was not analyzed in the three separate layers of nEB1 (indicated by nd).

endoderm, whereas the two internal layers (Table 1, L2 and L3) expressed markers of pluripotency. Immunofluorescence analysis of sectioned type 1 EBs showed clearly that αFP was expressed by the outside layer and Oct-4 by the inside layers (Fig. 4E). H19 expression was also detected in the outside layer by RT–PCR and in situ hybridization (Table 1, Fig. 4D). Types 3, 4, and 5 EBs expressed a mixture of VE and pluripotency markers (Table 1). Analysis of Oct-4 expression in these EB types by immunofluorescence or by in situ hybridization showed the presence of variable numbers of pluripotency marker-expressing cells in the various EB types (data not shown); moreover, αFP protein was detected in their outside layer. The presence of both VE-like and pluripotent marker-expressing cells in types 3, 4, and 5 EBs suggests that they represent intermediate stages in the development of the complex, multilayered structure of type 1 EBs.

In view of the importance of the visceral endoderm layer in the anterior–posterior development of mammalian embryos (reviewed by Perea-Gomez et al., 2001b), we examined in further detail the molecular identity of the outer layer of Nodal-expressing EBs using RT–PCR to detect the expression of genes typically expressed in the anterior visceral endoderm (AVE) of mouse embryos at the time of gastrulation (Bielinska et al., 1999). The outside layer of type 1 EBs expressed Hex, Lhx1, Cer, H19, and OTX2, which were not expressed by control EBs (Table 1, Fig. 4D). The most informative of these, Hex, which is a specific marker of the AVE in gastrulating mouse embryos, was expressed exclusively in the outer layer (Table 1). These results show that the molecular phenotype of the VE generated during Nodal-expressing EB development strikingly resembles that of the anterior visceral endoderm of mouse embryos.

We then investigated further the nature of the inner layers. The columnar organization of the inside layer strikingly resembled the epiblast layer of mouse embryos. Moreover, OTX2 was expressed in the inner layer and central core of Nodal-expressing EBs but not in undifferentiated hESCs (Table 1, Figs. 5A, B). During mouse embryo development, OTX2 is expressed just after implantation in visceral endoderm but is coexpressed with Oct-4 only in epiblast cells (Ang et al., 1994), suggesting that OTX2-expressing cells in Nodal-expressing EBs are indeed epiblast-like. To confirm this possibility, we examined the expression of well-characterized marker genes for mouse embryo development at the inner cell mass stage (GBX2; Chapman et al., 1997), the primitive ectoderm stage (FGF5; Rathjen et al., 1999), and the early epiblast stage (OTX2, Ang et al., 1994) during differentiation of wild-type or Nodal-expressing hESCs. We found that wild-type cells expressed GBX2 but neither OTX2 nor FGF5 (Figs. 5A, B), suggesting that they share certain transcriptional features of mouse inner cell mass cells. FGF5 expression was induced in wild-type EBs after 5 days of differentiation in CDM, while Oct4 disappeared and Neurod1 started to be expressed (Fig. 5A). GBX2 expression was maintained until day 14, which was not unexpected, given that GBX2 is also expressed in neuronal precursors after gastrulation (Wassarman et al., 1997). Thus, wild-type EBs appeared to undergo differentiation into a primitive ectoderm-like cell type expressing FGF5 before progressing towards a neuroectoderm-like cell type expressing Neurod1. By contrast, Nodal-expressing cells did not express FGF5 during differ-

entiation, and GBX2 was detected only in the outside layer of AVE-like cells of type 1 Nodal-expressing EBs (Figs. 5A, B). As expected, OTX2 was strongly expressed in the AVE layer, but it was also detected in the two inner layers (Table 1, Fig. 5B). These data suggest that hESC differentiation is blocked at an intermediate stage between inner cell mass and late epiblast as a consequence of Nodal expression during EB development in CDM. Finally, the differentiation of epiblast-like and AVE-like cell layers in Nodal-expressing EBs (both striking in their resemblance to mouse embryo cell lineages) appeared to be interdependent, as they were consistently found to be adjacent to each other (e.g., types 1 and 4 EBs). This could be explained on the basis of interactions between the AVE and epiblast layers as previously demonstrated in mouse embryos (reviewed in Perea-Gomez et al., 2001b), where AVE affects the progression of epiblast differentiation.

Nodal expression blocks differentiation of hESCs grown in adherent conditions in chemically defined medium

The developmental capacity of type 1 Nodal-expressing EBs was examined by growing them in adherent conditions, which fostered the outgrowth of their constituent cells. The first cells emerging from the spreading EBs within a few days of adherent culture (Fig. 5C) had a characteristic morphology with a flat nucleus and a large number of pinocytotic vacuoles, thereby resembling mouse AVE (Kimura et al., 2000). The extraembryonic endodermal phenotype of these cells was confirmed by the presence of large quantities of αFP protein (Fig. 5C). After 1 week in culture, a second cell type began to emerge: these were round with a small amount of cytoplasm and a large nucleus, and they grew as extensive monolayers similar to the early primitive ectoderm cells described by Rathjen et al. (1999) (Fig. 5C). These latter cells, evidently derived from the epiblast-like cell layer, expressed Oct-4 and Tra-1-60 (Figs. 5C, Supplementary Fig. 2), and they could be grown in adherent conditions for at least 10 passages (>50 days; data not shown). The source of these two distinct outgrowing cell types from the AVE-like outer layer and epiblast-like inner layer, respectively, was confirmed by microdissection and culture of isolated layers (data not shown). Expression of definitive neuroectoderm markers (Supplementary Fig. 2: NeuroD1) and mesoderm markers (Supplementary Fig. 2: MyoD, Myf5) was not detected by RT–PCR in the outgrowths from Nodal-expressing EBs, although these transcripts were seen in outgrowths from wild-type EBs (Supplementary Fig. 2 and data not shown). Expression of the definitive endoderm marker IFABP (Supplementary Fig. 2) was not detected in outgrowths from either Nodal-expressing or wild-type plated EBs. Therefore, differentiation of Nodal-expressing cells along each of the three definitive germ layer pathways seemed to be blocked when they were grown in adherent conditions.

To investigate this phenomenon further, we compared pluripotency marker gene expression in wild-type and Nodal-expressing hESCs that were grown directly in adherent conditions (i.e., without an EB intermediate phase) in CDM without FGF or serum. Under these conditions, wild-type hESCs began differentiating after the first passage, while Nodal-expressing hESCs formed large monolayers of cells resembling those outgrowing from type 1 Nodal-expressing EBs (data not shown; see Fig. 5C for illustration of this phenotype). These cells expressed Oct-4, SSEA-3, SSEA-4, and Tra-1-60 but not SSEA-1, a specific maker for differentiated cells (Fig. 5D and data not shown). The level of differentiation under these culture conditions was quantified by FACS, evaluating the fraction of cells expressing SSEA-4 or Tra-1-60 (Fig. 5D and data not shown). After six passages, 90% of the Nodal-expressing cells were SSEA-4-positive as compared to 17% for wild-type cells. In parallel cultures of wild-type hESCs grown on feeders, 95% were SSEA-4-positive. Similar results were obtained for Tra-1-60 expression (data not shown). Therefore, differentiation was blocked with a phenotype resembling that attained in EBs when Nodal-expressing hESCs were grown directly in adherent conditions for prolonged periods in culture. Interestingly, alpha-fetoprotein expression was rarely detected in these culture conditions showing that AVE-like cells were absent also suggesting that the emergence of the AVE phenotype depends on interactions that take place during EB development.

Nodal effects on EB development are position- and concentration-dependent

The distinct developmental fates of cells occupying the inner and outer regions of Nodal-expressing EBs could be explained by two different mechanisms. On the one hand, cells expressing different levels of Nodal could have moved during EB development to distinct regions of the EBs to form either the AVE-like outer layer or the epiblast-like inner layer (cell movement hypothesis). Alternatively, cells located on the outside of the EBs could have been induced to differentiate into VE owing their specific location in the EB's outer environment (inside/outside hypothesis). To distinguish between these two hypotheses, we mixed Nodal-expressing hESCs with green fluorescent hESCs (not Nodal-expressing) and then induced their differentiation by EB formation. The cell movement hypothesis predicted that Nodal-negative cells (i.e., GFP-positive cells) would be detected mainly or exclusively in one of the layers. This pattern was not observed, and instead green fluorescent cells were found throughout all three layers of type 1 EBs (nEB1, Fig. 6A). This result supports the view that distinct cell types differentiate in Nodal-expressing EBs as a result of their location.

Interestingly, the fraction of type 5 EBs (wild type-like) in these mixing experiments was greatly increased at the expense of the type 1 EB fraction (nEB1, Figs. 6A, B), just

as it was for NodalGFP expression EBs (Fig. 4B). Apparently, the dilution of Nodal-expressing cells by Nodal-nonexpressing cells provoked this shift in EB morphology. Consistent with this, EBs containing predominately green fluorescent cells generally developed with type 5 morphology and had a large fraction of Oct-4-negative cells (nEB5, Figs. 6A, B). However, when the type 1 EBs that did form in this series were examined by immuno-

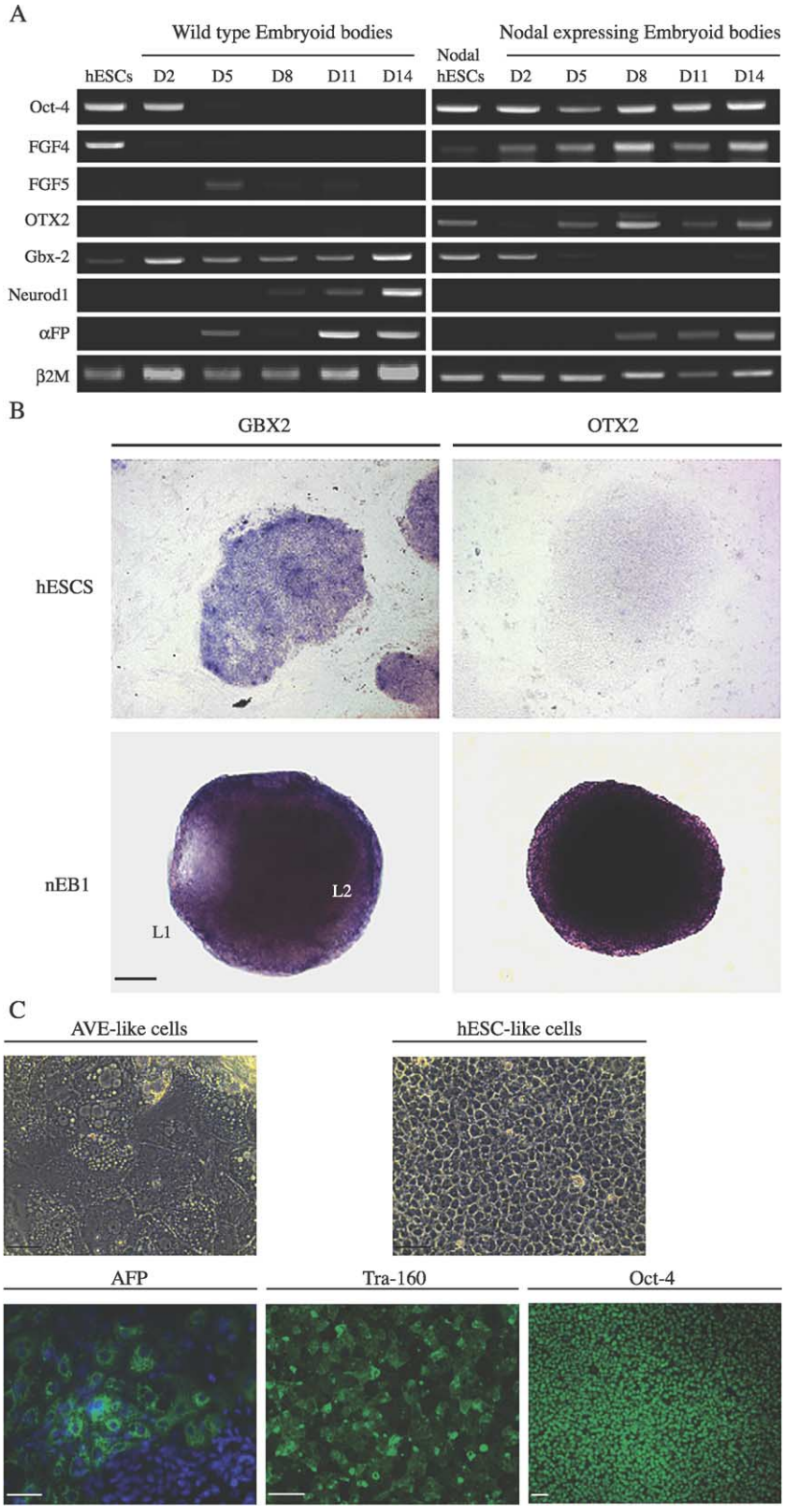

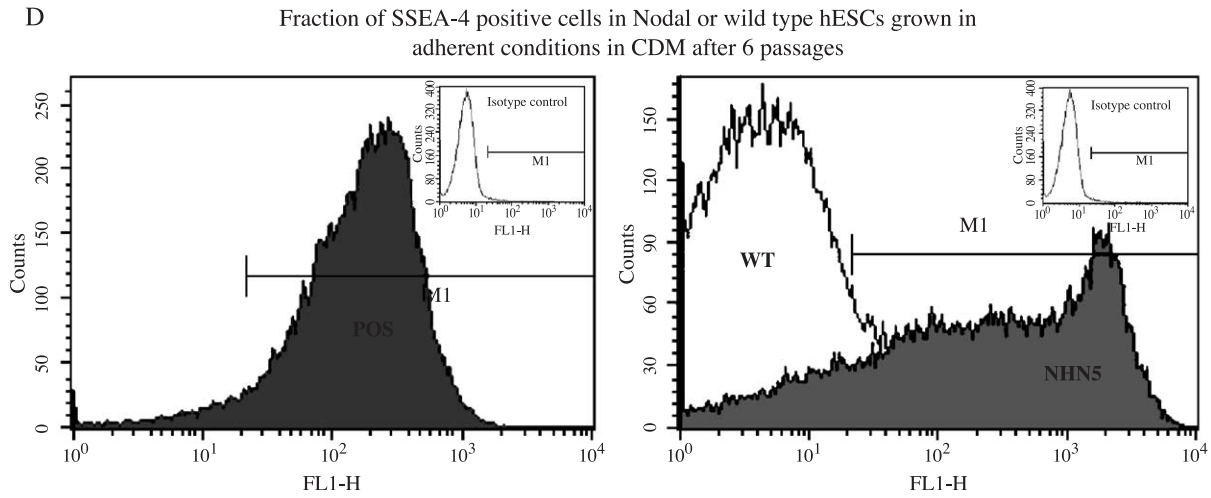

Fig. 5. Nodal blocks differentiation of hESCs at an early epiblast stage. (A) Examination of ICM and epiblast markers in hESCs and during differentiation using RT–PCR. Nodal-expressing cells or wild-type cells were grown in nonadherent conditions in CDM during 14 days. RNAs were extracted from EBs every 3 days, and RT–PCR analysis was performed to detect the expression of the genes denoted. (B) Analysis of GBX2 and OTX2 expression in hESCs (left and right top panels, respectively) and after 10 days of differentiation in Nodal-expressing EBs (bottom panels) using in situ hybridization. GBX2 was invariably detected in the outside layer (L1) of type 1 Nodal-expressing EBs (nEB1), but it was consistently absent from the inside layer (L2, left panel). OTX2 was expressed in the outside and inside layers (right panel). Scale bar: 100 μm. (C) Cells generated after plating of Nodal-expressing EBs. Morphology of AVE-like cells (left panel) and hESC-like cells (right panel) after 10 days of culture in adherent conditions. AVE-like cells expressed αFP (green fluorescence, bottom left panel), and hESC-like cells expressed Tra-1-60 and Oct-4 (green fluorescence, middle and right bottom panels). Scale bar: 50 μm. (D) Level of differentiation of wild-type hESCs (WT, right panel) or Nodal-expressing hESCs (NHN5, right panel) grown in adherent conditions in CDM was established using FACS to determine the fraction of SSEA-4-expressing cells after six passages (approximately 30 days). hESCs grown on feeders layer were used as positive control (Pos, left panel). Similar results were obtained with five different Nodal-expressing cell lines as with epiblast-like cells outgrowing from plating of Nodal-expressing EBs.

fluorescence, their green fluorescent cells (between 5% and 75% of total cells) were occasionally found to express Oct-4 if they were located in the inside layers. Taken together, these observations demonstrate that Nodal effects are concentration-dependent and that Nodal is able to affect neighboring cells (i.e., to act cell nonautonomously). Moreover, it is apparent from these mixing experiments that the Nodal generated by Nodal-expressing hESC acts predominantly locally within the embryoid bodies instead of by accumulating in the culture medium, since the Nodal-nonexpressing, Oct-4-positive cells were distributed in scattered, rather than continuous, patterns. This finding can account for the distinct phenotypes observed when Nodal was provided as exogenous recombinant, versus endogenously synthesized, protein.

Discussion

By treating hESCs with the TGF-β family member Nodal, either as recombinant protein or through expression of the mouse Nodal gene, we found that Nodal had dynamic effects on their in vitro development as EBs. Essentially, Nodal acted as an inducer of visceral endoderm and maintained the expression of known markers of pluripotency, two developmental outcomes that are likely to be interrelated. To place these effects in the context of normal mammalian development, it is worthwhile considering the role of Nodal in early mouse embryogenesis, since human embryos have not yet been studied in molecular detail at the corresponding developmental stages. This comparison illustrates the potential utility of hESCs in modeling human embryogenesis by providing insight into the role of Nodal in early human developmental events.

Nodal maintains expression of markers of pluripotency during differentiation of hESCs

During mouse development, Nodal expression is first detected just after implantation (5.5 dpc) throughout the epiblast and at lower levels in the surrounding layer of VE (Varlet et al., 1997). Nodal expression becomes restricted to the posterior part of the epiblast with the approach of gastrulation and disappears from the epiblast during primitive streak elongation, to be detected thereafter in the node and subsequently in the left lateral plate mesoderm (Collignon et al., 1996). This pattern of Nodal expression could indicate different functions for Nodal before and after gastrulation in mammals. Nodal null mutant embryos by themselves do not clarify this question because their growth is arrested before primitive streak formation (Conlon et al., 1994; Iannaccone et al., 1992; Zhou et al., 1993).

In addition to Nodal effects on axial patterning of the gastrula and later stage embryo, several features of both mouse embryos and hESCs suggest that Nodal signaling could also be involved in maintenance of pluripotency at

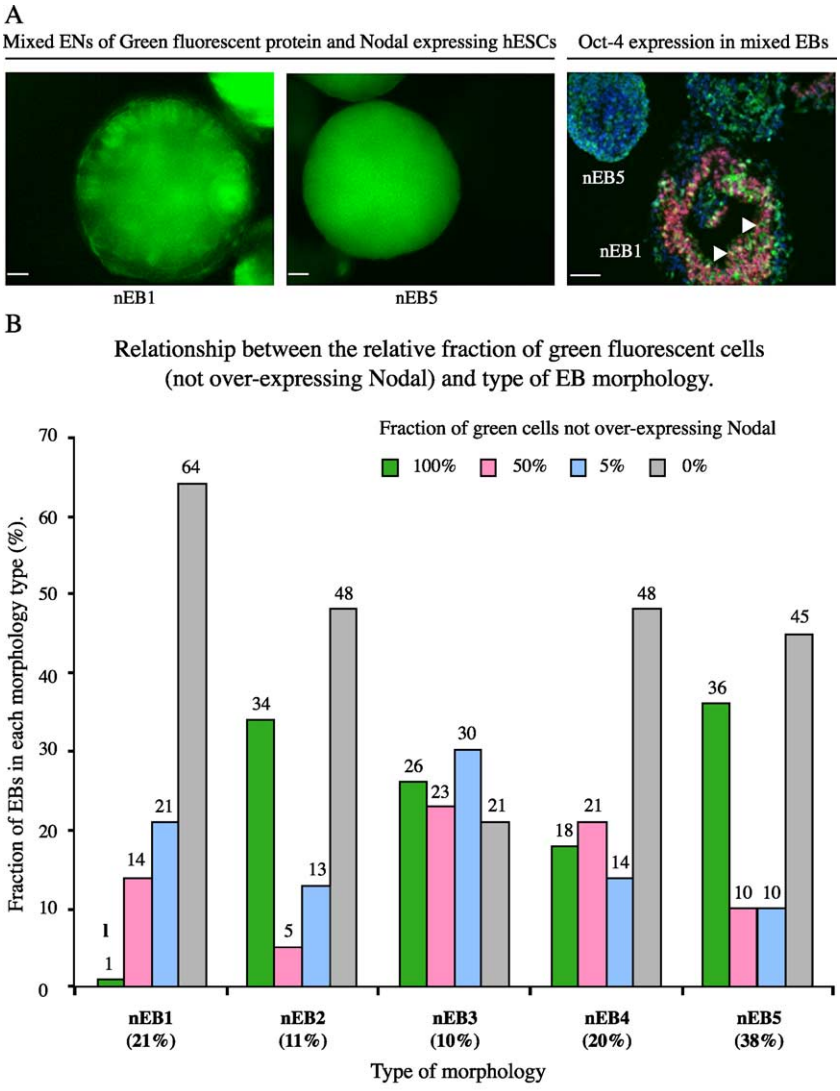

Fig. 6. Analysis of cell–cell interaction requirement for Nodal effect on pluripotency. (A) EBs generated from mixed colonies of green fluorescent hESCs (not Nodal-expressing) and Nodal-expressing hESCs. Left panel: type 1 EB (nEB1) generated after 10 days of differentiation showing the presence of green fluorescent cells in all three layers (whole mount). Middle panel type 5 EB (nEB5) containing only green fluorescent cells (whole mount). Right panel, immunofluorescence analysis of Oct-4 expression (red fluorescence) in a cryosectioned type 1 EB containing both nongreen and green fluorescent cells (nEB1) and of a type 5 EB containing only green fluorescent cells (nEB5). Blue fluorescence shows nuclei stained with Hoechst dye; blue/green fluorescence shows nuclei of green fluorescent protein expressing cells; pink fluorescence shows Oct-4 expression in Nodal expressing cells (red + blue); and yellow fluorescence (white arrow) shows Oct-4 expression in green fluorescent cells (red + green). Scale bar: 50 μm. (B) Relationship between the relative abundance of green fluorescent cells (i.e. not overexpressing Nodal) and type of morphology. Each type of EB (nEB1–nEB5) was divided into four different arbitrary categories based on the relative amount of green fluorescent cells they contained (0%, approximately 5%, approximately 50%, approximately 100%). This experiment was repeated three times and similar results were obtained. Thus, results were pooled, with the fraction number of EBs in each category indicated in parentheses (number of EBs in each subclass indicated at top of histogram bars).

earlier stages. Specifically, mouse Nodal null mutants display very low levels of Oct-4 expression, and the size of the epiblast cell population is substantially reduced (Conlon et al., 1994; Iannaccone et al., 1992; Robertson et al., 2003). From this perspective, the pregastrulation arrest of Nodal null mutant mouse embryos could reflect the diminished capacity of Nodal-deficient epiblast cells for self-renewal, rather than a blockade in the induction of mesoderm and endoderm precursors. Thus, the absence of posterior markers (i.e., Wnt3 and FGF8) in Nodal null mouse embryos (Brennan et al., 2001; Robertson et al., 2003) could be understood as a consequence of diminished pluripotency. Applied to early human development, this hypothesis appears to be supported by our experiments, since hESC differentiation is blocked by Nodal over-expression, as revealed by the continued expression of markers of pluripotency in hESC cultured with recNodal or expressing Nodal.

While the expression pattern of Nodal and its receptor-mediated signaling pathway are unknown in peri-implantation human embryos, the onset of Nodal expression in mouse embryos (E5.5, specifically in epiblast) suggests a

unique role of Nodal in epiblast development. Consistently with this suggestion, one prominent response to Nodal expression in hESCs is development of a pluripotent cell layer with striking morphological and molecular resemblance to epiblast. The hESC-like monolayers generated by plating Nodal-expressing EBs also share some morphological characteristics with mouse early primitive ectoderm cells, in that they grow in large monolayer colonies and have a small amount of cytoplasm, somewhat similar to the EPL cells reported by Rathjen et al. (1999). However, such Nodal-expressing EB-derived cells have a distinct molecular signature from primitive ectoderm (Rodda et al., 2002), in that they do not express FGF-5. While it remains difficult to establish the equivalence between hESC-derived and true embryo-derived lineages without the early human embryo gene expression patterns for comparison, it nevertheless appears that the epiblast-like inner (L2) layer of Nodal-expressing EBs represents a cell type that is distinct from the inner cell mass of blastocysts, yet has not progressed to the onset of epiblast differentiation that accompanies gastrulation. This cell type could have unique features in human embryos, since the time between implantation and gastrulation is significantly longer than in the mouse.

Taken together, these results suggest that Nodal functions to maintain pluripotency in Nodal-expressing EBs in a cell type equivalent to the epiblast layer, or its more primitive precursor, in the mammalian embryo before gastrulation (Fig. 7, model A). The absence of definitive mesoderm or endoderm differentiation in Nodal-treated or Nodal-expressing hESCs seems to be in contradiction with results obtained in chick (Bertocchini and Stern, 2002), *Xenopus* (Jones et al., 1995), zebrafish (Erter et al., 1998), and in mouse (Perea-Gomez et al., 2002) embryos, where Nodal gain of function enhances mesendoderm development. However, those experiments were done during gastrulation in vivo, where additional growth factors (e.g., BMP-4, Wnt-3, FGF-4, -5, -8) that could synergize with Nodal are also present. The chemically defined medium used in the present study, by contrast, contains only factors produced by the cells themselves and so might not be sufficient to provoke mesendoderm differentiation. However, when Nodal-expressing EBs were cultured in medium containing FBS, which should provide additional factors needed for differentiation, they continued to express markers of pluripotency (data not shown). Therefore, promotion of pluripotency, rather than definitive germ layer differentiation, appeared to be the dominant consequence of Nodal expression in the hESC system. It should be noted that Nodal may have different consequences for each particular stage of epiblast development, in which case the intermediate stage apparently formed by Nodal-expressing EBs could be less responsive to Nodal-induced mesoderm and endoderm differentiation than epiblast cells at the threshold of gastrulation.

Our findings of Nodal-induced maintenance of pluripotency could reflect either the direct action of Nodal on

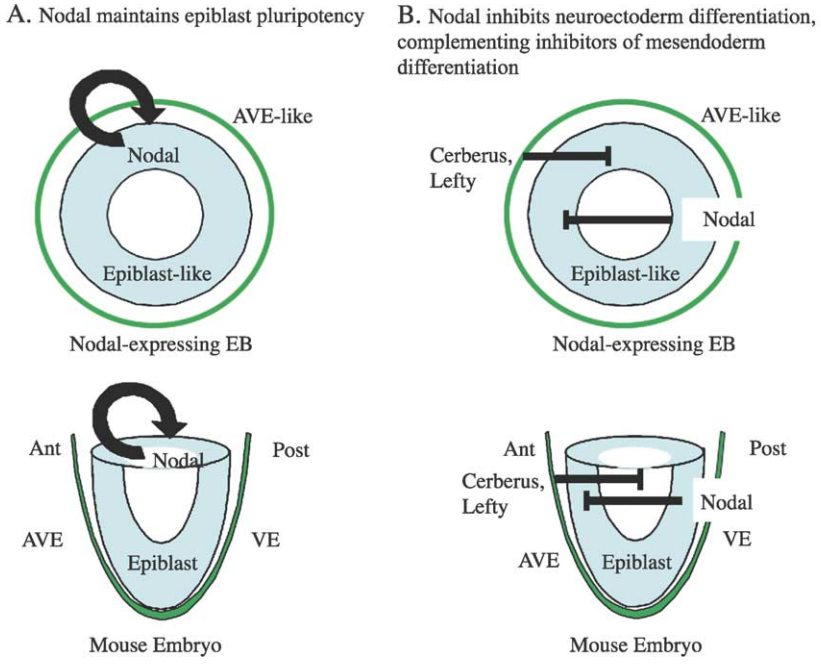

Fig. 7. Alternative models for Nodal effects on development of the epiblast-like layer of Nodal-expressing EBs and the epiblast cells of mouse embryos. (Model A) Nodal maintains pluripotency through direct effects on epiblast-like and epiblast cells. (Model B) Nodal-induced differentiation of AVE-like cells leads to secretion of inhibitors (e.g., Cerberus, Lefty) of mesoderm and endoderm differentiation; Nodal prevents neuroectoderm differentiation through direct effects on epiblast-like and epiblast cells. The net effect in either case is maintenance of pluripotency by epiblast-like cells of Nodal-expressing hESC EBs. Comparable mechanisms in mouse embryos would lead to maintenance of epiblast pluripotency (model A) or polarized anterior–posterior development of epiblast (model B). Ant indicates anterior; Post, posterior; VE, visceral endoderm; AVE, anterior visceral endoderm.

pluripotent cells or alternatively could represent an indirect mechanism in which pluripotency is maintained through Nodal-induced differentiation of extraembryonic tissues.

Nodal induction of AVE-like differentiation and its potential for inhibition of mesoderm and endoderm differentiation

Nodal expression by hESC during EB development induces the differentiation of an outer layer of AVE-like cells, as evidenced by expression of the AVE markers Hex, Cer, and OTX2 (Ang et al., 1994; Shawlot et al., 1998; Thomas et al., 1998). While these markers are also expressed in the anterior definitive endoderm of mouse embryos, the outer cells of Nodal-expressing EBs homogenously express αFP and H19, two distinctive markers of extraembryonic endoderm in the mouse (Krumlauf et al., 1985; Poirier et al., 1991). Thus, Nodal signaling appears to be sufficient to initiate and sustain the differentiation of an AVE-like phenotype.

Previous studies on mouse embryos have revealed an essential function for Nodal in differentiation of the AVE and, through it, on anterior–posterior patterning. Chimeric analysis using wild-type mouse ES cells to rescue Nodal mutant mouse embryos has demonstrated that absence of Nodal expression in prospective VE induces truncation of the anterior regions (Varlet et al., 1997). Moreover, hypomorphic mutations and deletions of specific enhancers within the regulatory region of the Nodal gene allow development to proceed through gastrulation and reveal the distinct roles of early and later phases of Nodal signaling (Lowe et al., 2001; Norris et al., 2002; Robertson et al., 2003). Those studies show that expression of Nodal in mouse embryos is needed not only for initiation of gastrulation, but also for the normal development of the VE, notably for the stereotypic anterior movement of the VE that precedes and accompanies gastrulation and is necessary for acquisition of anterior–posterior polarity (Yamamoto et al., 2004; reviewed in Perea-Gomez et al., 2001b). These and other developmental consequences of Nodal expression are highly dose-dependent, as revealed by the different spectrum of phenotypes depending on the level of Nodal actually produced (Lowe et al., 2001; Norris et al., 2002).

It is well established that AVE and anterior definitive endoderm (ADE) of the mouse embryo secrete factors that inhibit the function of posteriorizing signals (reviewed in Perea-Gomez et al., 2001b). Cerberus and Lefty are the principal inhibitors of Nodal function that are known to act during gastrulation (Belo et al., 1997; Meno et al., 1999). Double mutants for these two genes develop several primitive streaks; nevertheless, they also express neuronal markers, so the AVE does not appear to act as an inhibitor of neuroectoderm development (Perea-Gomez et al., 2002). Germ layer explant assays combining ectoderm and VE have also shown that mouse AVE is capable of acting as an inhibitor of posteriorizing signals (Kimura et al., 2000). The strength of evidence in support of an AVE-dependent mechanism for inhibition of posteriorizing signals leads us to postulate that the presence of an AVE-like layer surrounding Nodal-expressing EBs contributes to blocking the induction of mesoderm and endoderm differentiation. However, maintenance of pluripotency markers cannot be explained by this mechanism alone. This is because the neuroectoderm default model (reviewed in Munoz-Sanjuan and Brivanlou, 2002) applies to the hESC system and should thus lead the inner cells of Nodal-expressing EBs to adopt a neuroectoderm fate even in the presence of AVE. Since this was not observed, Nodal would appear to act directly either to maintain pluripotency or to inhibit neuronal differentiation (Fig. 7, model B). Such a mechanism would be in agreement with the recent model of pluripotency proposed by Ying et al. (2003) for mouse ES cells, postulating that self-renewal is the result of two distinctive differentiation-inhibiting signals, one preventing mesendoderm formation and another neuroectoderm.

The possibility that Nodal is able to inhibit neuronal differentiation is supported by the null mutation of the transcriptional corepressor Drap1 (Iratni et al., 2002), which induces abnormal expression of Nodal in the anterior part of the embryo before gastrulation, blocks expression of anterior neuroectoderm markers, and causes ectopic expression of posterior markers. Thus, it appears likely that Nodal function can directly interfere with neuroectoderm development at early stages of development (i.e., before primitive streak formation). In exploring this hypothesis, we generated multiple hESC lines stably overexpressing either Lefty (n = 24) or Cerberus-Short (n = 32) (L. Vallier and R.A. Pedersen, unpublished observations). Preliminary examination of representative lines shows that such inhibition of Nodal function in these lines does not provoke hESC differentiation, suggesting that Nodal acts jointly with other factor(s) in maintaining pluripotency. TGFβ1 and Activin are potential candidates, since they can both activate the same signaling pathway as Nodal. Intriguingly, these Lefty- and Cerberus-Short-expressing hESC lines underwent extensive neuroectodermal development, consistent with our findings on Nodal gain-of-function in which neurectoderm development was inhibited. Further experiments analyzing the TGFβ signaling pathway at the molecular level in hESCs will provide essential details on mechanisms involving Nodal both in maintaining pluripotency and inhibiting neural development.

Taken together with mouse loss-of-function studies, our findings lead to the view (Fig. 7) that the posterior region of the mammalian embryo, with its posteriorly localized expression of Nodal (and other factors), acts to inhibit anterior patterning reciprocally to the AVE and ADE (with their inhibitory effect on posterior patterning). Further in vivo experiments with mouse embryos will be needed to evaluate this hypothesis.

The potential for clinical applications of hESCs is promising, and thus the control of their differentiation is a major focus of current stem cell research. Because hES cells

are capable of undergoing differentiation into the primary germ layers and their derivatives, they also represent a unique in vitro model to study the earliest events in human development. Despite the limitations imposed by the absence of data from corresponding stages of human embryos, the comparison of our findings with the intact mouse embryo provides evidence for the potential value of this approach. Our results showing Nodal-induced AVE differentiation may indicate that this extraembryonic lineage is involved in anterior–posterior patterning in human development through similar mechanisms as it is in the mouse. Thus, a combination of hESC and animal modeling can provide a powerful approach for understanding molecular mechanisms regulating the first events of differentiation during gastrulation in mammals, including humans. In turn, such studies will lead to the design of novel strategies for directing differentiation of hESCs into fully functional cell types, thus revealing their potential for clinical application.

Acknowledgments

We thank M. Alexander for her exemplary support in cell culture, M.R. Kuehn and K. Pfendler for the Nodal cDNA and the mouse Nodal primers, T. Pratt for the pTp6 vector, H. Hamada for the NoGFP fusion gene, J. Wrana for the PAR3-lux reporter, P.W. Andrews for the TRA-1-60 antibody, J.A. Thomson and Wicell for H9 cells, M. Firpo for providing access to ES cells and protocols, P.J. Rugg-Gunn for the H19 in situ, and K. Bowles for his contribution regarding flow cytometry. The SSEA-1 and SSEA-4 antibodies were obtained from the Developmental Hybridoma Bank. We are grateful to Dr. S.L. Ang for her helpful comments on the manuscript. This work was supported by the Medical Research Council and the Human Frontiers Science Program.

Appendix A. Supplementary data

Supplementary data associated with this article can be found, in the online version, at doi:10.1016/j.ydbio.2004.08.031.

References

Amit, M., Carpenter, M.K., Inokuma, M.S., Chiu, C.P., Harris, C.P., Waknitz, M.A., Itskovitz-Eldor, J., Thomson, J.A., 2000. Clonally derived human embryonic stem cell lines maintain pluripotency and proliferative potential for prolonged periods of culture. Dev. Biol. 227 (2), 271–278.

Ang, S.L., Conlon, R.A., Jin, O., Rossant, J., 1994. Positive and negative signals from mesoderm regulate the expression of mouse Otx2 in ectoderm explants. Development 120, 2979–2989.

Avilion, A.A., Nicolis, S.K., Pevny, L.H., Perez, L., Vivian, N., Lovell-Badge, R., 2003. Multipotent cell lineages in early mouse development depend on SOX2 function. Genes Dev. 17 (1), 126–140.

Belo, J.A., Bouwmeester, T., Leyns, L., Kertesz, N., Gallo, M., Follettie, M., De Robertis, E.M., 1997. Cerberus-like is a secreted factor with neutralizing activity expressed in the anterior primitive endoderm of the mouse gastrula. Mech. Dev. 68, 45–57.

Bertocchini, F., Stern, C.D., 2002. Hypoblast of the chick embryo positions the primitive streak by antagonizing nodal signaling. Dev. Cell 3, 735–744.

Bielinska, M., Narita, N., Wilson, D.B., 1999. Distinct roles for visceral endoderm during embryonic mouse development. Int. J. Dev. Biol. 43, 183–205.

Brandenberger, R., Wei, H., Zhang, S., Lei, S., Murage, J., Fisk, G.J., Li, Y., Xu, C., Fang, R., Guegler, K., Rao, M.S., Mandalam, R., Lebkowski, J., Stanton, L.W., 2004. Transcriptome characterization elucidates signaling networks that control human ES cell growth and differentiation. Nat. Biotechnol. 22, 707–716.

Brennan, J., Lu, C.C., Norris, D.P., Rodriguez, T.A., Beddington, R.S., Robertson, E.J., 2001. Nodal signalling in the epiblast patterns the early mouse embryo. Nature 411, 965–969.

Breslin, M.B., Zhu, M., Lan, M.S., 2003. NeuroD1/E47 regulates the E-box element of a novel zinc finger transcription factor, IA-1, in developing nervous system. J. Biol. Chem. 278, 38991–38997.

Brivanlou, A.H., Gage, F.H., Jaenisch, R., Jessell, T., Melton, D., Rossant, J., 2003. Related stem cells. Setting standards for human embryonic stem cells. Science 300, 913–916.

Chapman, G., Remiszewski, J.L., Webb, G.C., Schulz, T.C., Bottema, C.D., Rathjen, P.D., 1997. The mouse homeobox gene, *Gbx2*: genomic organization and expression in pluripotent cells in vitro and in vivo. Genomics 46, 223–233.

Collignon, J., Varlet, I., Robertson, E.J., 1996. Relationship between asymmetric nodal expression and the direction of embryonic turning. Nature 381, 155–158.

Conlon, F.L., Lyons, K.M., Takaesu, N., Barth, K.S., Kispert, A., Herrmann, B., Robertson, E.J., 1994. A primary requirement for nodal in the formation and maintenance of the primitive streak in the mouse. Development 120, 1919–1928.

Constam, D.B., Robertson, E.J., 1999. Regulation of bone morphogenetic protein activity by pro domains and proprotein convertases. J. Cell Biol. 144, 139–149.

Dale, L., Matthews, G., Colman, A., 1993. Secretion and mesoderm-inducing activity of the TGF-related domain of *Xenopus* Vg1. EMBO J. 12, 4471–4480.

Draper, J.S., Smith, K., Gokhale, P., Moore, H.D., Maltby, E., Johnson, J., Meisner, L., Zwaka, T.P., Thomson, J.A., Andrews, P.W., 2004. Recurrent gain of chromosomes 17q and 12 in cultured human embryonic stem cells. Nat. Biotechnol. 22, 53–54.

Erter, C.E., Solnica-Krezel, L., Wright, C.V.E., 1998. Zebrafish nodal-related 2 encodes an early mesendodermal inducer signaling from the extraembryonic yolk syncytial layer. Dev. Biol. 204, 361–372.

Ginis, I., Luo, Y., Miura, T., Thies, S., Brandenberger, R., Gerecht-Nir, S., Amit, M., Hoke, A., Carpenter, M.K., Itskovitz-Eldor, J., Rao, M.S., 2004. Differences between human and mouse embryonic stem cells. Dev. Biol. 269, 360–380.

Hallonet, M., Kaestner, K.H., Martin-Parras, L., Sasaki, H., Betz, U.A., Ang, S.L., 2002. Maintenance of the specification of the anterior definitive endoderm and forebrain depends on the axial mesendoderm: a study using HNF3beta/Foxa2 conditional mutants. Dev. Biol. 243, 20–33.

Hayashi, H., Abdollah, S., Qiu, Y., Cai, J., Xu, Y.Y., Grinnell, B.W., Richardson, M.A., Topper, J.N., Gimbrone Jr., M.A., Wrana, J.L., Falb, D., 1997. The MAD-related protein Smad7 associates with the TGFbeta receptor and functions as an antagonist of TGFbeta signaling. Cell 89, 1165–1173.

Henderson, J.K., Draper, J.S., Baillie, H.S., Fishel, S., Thomson, J.A., Moore, H., Andrews, P.W., 2002. Preimplantation human embryos and embryonic stem cells show comparable expression of stage-specific embryonic antigens. Stem Cells 20, 329–337.

Iannaccone, P.M., Zhou, X., Khokha, M., Boucher, D., Kuehn, M.R., 1992. Insertional mutation of a gene involved in growth regulation of the early mouse embryo. Dev. Dyn. 194, 198–208.

Iratni, R., Yan, Y.T., Chen, C., Ding, J., Zhang, Y., Price, S.M., Reinberg, D., Shen, M.M., 2002. Inhibition of excess nodal signaling during mouse gastrulation by the transcriptional corepressor DRAP1. Science 298, 1996–1999.

Johansson, B.M., Wiles, M.V., 1995. Evidence for involvement of Activin A and bone morphogenetic protein 4 in mammalian mesoderm and hematopoietic development. Mol. Cell. Biol. 15, 141–151.

Jones, C.M., Kuehn, M.R., Hogan, B.L., Smith, J.C., Wright, C.V., 1995. Nodal-related signals induce axial mesoderm and dorsalize mesoderm during gastrulation. Development 121, 3651–3662.

Kalantry, S., Manning, S., Haub, O., Tomihara-Newberger, C., Lee, H.G., Fangman, J., Disteche, C.M., Manova, K., Lacy, E., 2001. The amnionless gene, essential for mouse gastrulation, encodes a visceral-endoderm-specific protein with an extracellular cysteine-rich domain. Nat. Genet. 27, 412–416.

Kimura, C., Yoshinaga, K., Tian, E., Suzuki, M., Aizawa, S., Matsuo, I., 2000. Visceral endoderm mediates forebrain development by suppressing posteriorizing signals. Dev. Biol. 225, 304–321.

Krumlauf, R., Hammer, R.E., Tilghman, S.M., Brinster, R.L., 1985. Developmental regulation of alpha-fetoprotein genes in transgenic mice. Mol. Cell. Biol. 5, 1639–1648.

Kumar, A., Novoselov, V., Celeste, A.J., Wolfman, N.M., ten Dijke, P., Kuehn, M.R., 2001. Nodal signaling uses Activin and transforming growth factor-beta receptor-regulated Smads. J. Biol. Chem. 276, 656–661.

Lowe, L.A., Yamada, S., Kuehn, M.R., 2001. Genetic dissection of nodal function in patterning the mouse embryo. Development 128, 1831–1843.

Lu, C.C., Brennan, J., Robertson, E.J., 2001. From fertilization to gastrulation: axis formation in the mouse embryo. Curr. Opin. Genet. Dev. 11, 384–392.

Meno, C., Gritsman, K., Ohishi, S., Ohfuji, Y., Heckscher, E., Mochida, K., Shimono, A., Kondoh, H., Talbot, W.S., Robertson, E.J., et al., 1999. Mouse Lefty2 and zebrafish Activin are feedback inhibitors of nodal signalling during vertebrate gastrulation. Mol. Cell 4, 287–298.

Munoz-Sanjuan, I., Brivanlou, A.H., 2002. Neural induction, the default model and embryonic stem cells. Nat. Rev., Neurosci. 3, 271–280.

Narita, N., Bielinska, M., Wilson, D.B., 1997. Cardiomyocyte differentiation by GATA-4-deficient embryonic stem cells. Development 124, 3755–3764.

Norris, D.P., Brennan, J., Bikoff, E.K., Robertson, E.J., 2002. The FoxH1 dependent autoregulatory enhancer controls the level of Nodal signals in the mouse embryo. Development 129, 3455–3468.

Parisi, S., D'Andrea, D., Lago, C.T., Adamson, E.D., Persico, M.G., Minchiotti, G., 2003. Nodal-dependent Cripto signaling promotes cardiomyogenesis and redirects the neural fate of embryonic stem cells. J. Cell Biol. 163, 303–314.

Parker, M.H., Seale, P., Rudnicki, M.A., 2003. Looking back to the embryo: defining transcriptional networks in adult myogenesis. Nat. Rev., Genet. 4, 497–507.

Perea-Gomez, A., Lawson, K.A., Rhinn, M., Zakin, L., Brulet, P., Mazan, S., Ang, S.L., 2001a. Otx2 is required for visceral endoderm movement and for the restriction of posterior signals in the epiblast of the mouse embryo. Development 128, 753–765.

Perea-Gomez, A., Rhinn, M., Ang, S.L., 2001b. Role of the anterior visceral endoderm in restricting posterior signals in the mouse embryo. Int. J. Dev. Biol. 45, 311–320.

Perea-Gomez, A., Vella, F.D., Shawlot, W., Oulad-Abdelghani, M., Chazaud, C., Meno, C., Pfister, V., Chen, L., Robertson, E., Hamada, H., Behringer, R.R., Ang, S.L., 2002. Nodal antagonists in the anterior visceral endoderm prevent the formation of multiple primitive streaks. Dev. Cell 3, 745–756.

Poirier, F., Chan, C.T., Timmons, P.M., Robertson, E.J., Evans, M.J., Rigby, P.W., 1991. The murine H19 gene is activated during embryonic stem cell differentiation in vitro and at the time of implantation in the developing embryo. Development 113, 1105–1114.

Pratt, T., Sharp, L., Nichols, J., Price, D.J., Mason, J.O., 2000. Embryonic stem cells and transgenic mice ubiquitously expressing a tau-tagged green fluorescent protein. Dev. Biol. 228, 19–28.

Rathjen, J., Lake, J.A., Bettess, M.D., Washington, J.M., Chapman, G., Rathjen, P.D., 1999. Formation of a primitive ectoderm like cell population, EPL cells, from ES cells in response to biologically derived factors. J. Cell Sci. 112, 601–612.

Robertson, E.J., Norris, D.P., Brennan, J., Bikoff, E.K., 2003. Control of early anterior–posterior patterning in the mouse embryo by TGF-beta signalling. Philos. Trans. R. Soc. London, B Biol. Sci. 358, 1351–1357.

Rodda, S.J., Kavanagh, S.J., Rathjen, J., Rathjen, P.D., 2002. Embryonic stem cell differentiation and the analysis of mammalian development. Int. J. Dev. Biol. 46, 449–458.

Sakuma, R., Yi, Y., Meno, C., Fujii, H., Juan, H., Takeuchi, J., Ogura, T., Li, E., Miyazono, K., Hamada, H., 2002. Inhibition of Nodal signalling by Lefty mediated through interaction with common receptors and efficient diffusion. Genes Cells 7, 401–412.

Schier, A.F., 2003. Nodal signaling in vertebrate development. Annu. Rev. Cell Dev. Biol. 19, 589–621.

Schuldiner, M., Yanuka, O., Itskovitz-Eldor, J., Melton, D.A., Benvenisty, N., 2000. Effects of eight growth factors on the differentiation of cells derived from human embryonic stem cells. Proc. Natl. Acad. Sci. U. S. A. 97, 11307–11312.

Shawlot, W., Deng, J.M., Behringer, R.R., 1998. Expression of the mouse Cerberus-related gene, *Cerr1*, suggests a role in anterior neural induction and somitogenesis. Proc. Natl. Acad. Sci. U. S. A. 95, 6198–6203.

Streit, A., Stern, C.D., 2001. Combined whole-mount in situ hybridization and immunohistochemistry in avian embryos. Methods 23, 339–344.

Thomas, P.Q., Brown, A., Beddington, R.S.P., 1998. *Hex*: a homeobox gene revealing peri-implantation asymmetry in the mouse embryo and an early transient marker of endothelial cell precursors. Development 125, 85–94.

Thomsen, G.H., Melton, D.A., 1993. Processed Vg1 protein is an axial mesoderm inducer in *Xenopus*. Cell 74, 433–441.

Thomson, J.A., Itskovitz-Eldor, J., Shapiro, S.S., Waknitz, M.A., Swiergiel, J.J., Marshall, V.S., Jones, J.M., 1998. Embryonic stem cell lines derived from human blastocysts. Science 282, 1145–1147.

Tropepe, V., Hitoshi, S., Sirard, C., Mak, T.W., Rossant, J., van der Kooy, D., 2001. Direct neural fate specification from embryonic stem cells: a primitive mammalian neural stem cell stage acquired through a default mechanism. Neuron 30, 65–78.

Vallier, L., Rugg-Gunn, P.J., Bouhon, I.A., Andersson, F.K., Sadler, A.J., Pedersen, R.A., 2004. Enhancing and diminishing gene function in human embryonic stem cells. Stem Cells 22, 2–11.

Varlet, I., Collignon, J., Robertson, E.J., 1997. Nodal expression in the primitive endoderm is required for specification of the anterior axis during mouse gastrulation. Development 124, 1033–1044.

Wassarman, K.M., Lewandoski, M., Campbell, K., Joyner, A.L., Rubenstein, J.L., Martinez, S., Martin, G.R., 1997. Specification of the anterior hindbrain and establishment of a normal mid/hindbrain organizer is dependent on *Gbx2* gene function. Development 124, 2923–2934.

Wells, J.M., Melton, D.A., 2000. Early mouse endoderm is patterned by soluble factors from adjacent germ layers. Development 127, 1563–1572.

Wiles, M.V., Johansson, B.M., 1999. Embryonic stem cell development in a chemically defined medium. Exp. Cell Res. 247, 241–248.

Xu, R.H., Chen, X., Li, D.S., Li, R., Addicks, G.C., Glennon, C., Zwaka, T.P., Thomson, J.A., 2002. BMP4 initiates human embryonic stem cell differentiation to trophoblast. Nat. Biotechnol. 20, 1261–1264.

Yamamoto, M., Saijoh, Y., Perea-Gomez, A., Shawlot, N., Behringer, R.R., Ang, S.L., Hamada, H., Meno, C., 2004. Nodal antagonists regulate migration of the anteroposterior axis of the mouse embryo. Nature. 428, 387–392.

Ying, Q.L., Nichols, J., Chambers, I., Smith, A., 2003. BMP induction of Id proteins suppresses differentiation and sustains embryonic stem cell self-renewal in collaboration with STAT3. Cell 115, 281–292.

Zeng, X., Miura, T., Luo, Y., Bhattacharya, B., Condie, B., Chen, J., Ginis, I., Lyons, I., Mejido, J., Puri, R.K., Rao, M.S., Freed, W.J., 2004. Properties of pluripotent human embryonic stem cells BG01 and BG02. Stem Cells 22, 292–312.

Zhou, X., Sasaki, H., Lowe, L., Hogan, B.L., Kuehn, M.R., 1993. Nodal is a novel TGF-beta-like gene expressed in the mouse node during gastrulation. Nature 361, 543–547.